Eur. Phys. J. A **6**, 415–420 (1999)

THE EUROPEAN PHYSICAL JOURNAL A

Low-mass dileptons at the CERN-SpS: evidence for chiral restoration?

R. Rapp[1], J. Wambach[2]

[1] Department of Physics and Astronomy, State University of New York, Stony Brook, NY 11794-3800, USA
[2] Institut für Kernphysik, TU Darmstadt, Schlossgartenstr. 9, 64289 Darmstadt, Germany

Received: 30 September 1999
Communicated by B. Povh

Abstract. Using a rather complete description of the in-medium ρ spectral function – being constrained by various independent experimental information – we calculate pertinent dilepton production rates from hot and dense hadronic matter. The strong broadening of the ρ resonance entails a reminiscence to perturbative $q\bar{q}$ annihilation rates in the vicinity of the phase boundary. The application to dilepton observables in Pb(158AGeV)+Au collisions – incorporating recent information on the hadro-chemical composition at CERN-SpS energies – essentially supports the broadening scenario. Possible implications for the nature of chiral symmetry restoration are outlined.

PACS. 12.40.Vv Vector-meson dominance – 21.65.+f Nuclear matter

1 Introduction

In the low-energy sector ($q^2 \leq 1-2$ GeV^2) the properties of Quantum Chromodynamics are believed to be governed by (approximate) chiral symmetry and its dynamical breaking. In hot and dense matter as created through energetic collisions of heavy nuclei chiral symmetry is believed to be restored, associated with the disappearance of the chiral condensate and a substantial reshaping of the low-lying hadronic spectrum. As the chiral condensate does not represent a physical observable, the detection of signatures for chiral restoration has to focus on medium effects in hadronic properties. Dileptons as penetrating probes provide the opportunity to study rather directly the in-medium modifications of light vector mesons through their decays $V \to l^+l^-$.

Measurements of low-mass dilepton spectra in heavy-ion collisions at CERN-SpS energies [1,2] have revealed appreciable radiation beyond final-state hadron decays. However, the spectral shape of this additional contribution – stemming from the interaction phase of the hadronic fireball – is not easily accounted for. In particular, using the vacuum vector meson line shapes, the enhancement around $M_{ll} \simeq (0.2-0.6)$ GeV remains unexplained. At the same time the yield in the ρ/ω mass region tends to be overestimated. The central question then is whether one has possibly observed signatures of (the onset of) chiral symmetry restoration, and, if so, *how* it manifests itself in the vector channel.

Several theoretical approaches have been pursued to study medium effects in dilepton production rates from hot/dense matter, e.g., the 'dropping rho mass' scenario (within a mean-field type treatment) [3–5], the chiral reduction formalism (based on chiral Ward identities in connection with low-density expansions) [6], chiral Lagrangian frameworks [7] or many-body-type calculations of in-medium vector-meson spectral functions [8–11], see also [12] for a recent review. As a further complication, the quantitative impact of in-medium effects on the final spectra depends on another important ingredient, namely the modeling of the space-time evolution of the global heavy-ion collision dynamics. Here, transport calculations seem to give substantially larger dilepton yields than hydrodynamic simulations. A reason for this discrepancy might be related to an overpopulation of pion phase space (enhancing the $\pi\pi \to \rho \to ll$ annihilation contribution).

In the present article we will focus on the in-medium spectral function approach for the elementary dilepton production processes, presenting its most recent developments, thereby noting a surprising reminiscence to (perturbative) quark-based calculations. We then apply the medium-modified dilepton rates to the calculation of spectra from $\pi\pi \to \rho \to ee$ annihilation in 30% central Pb(158 AGeV)+Au collisions and perform a detailed comparison to various projections of the recent data from the CERES/NA45 collaboration. Special care is taken to adopt a realistic temperature/density profile of the collision dynamics using a thermal fireball expansion with a particle composition consistent with recent hadro-chemical analyses at SpS energies [13,14]. The subsequent evolution towards thermal freezeout is determined by assuming entropy as well as pion- and kaon-number con-

servation which induces the build-up of finite pion-/kaon-chemical potentials [15].

2 Production rates in hot/dense matter

The radiation of dileptons from a hot and dense medium characterized by a temperature T and baryon chemical potential μ_B,

$$\frac{d^8N_{l^+l^-}}{d^4xd^4q} = -\frac{\alpha^2}{\pi^3 M^2}\, f^B(q_0;T)\, \mathrm{Im}\Pi_{\mathrm{em}}(q_0,\boldsymbol{q};\mu_B,T)\ , \quad (1)$$

is governed by the thermal expectation value of the (retarded) electromagnetic (e.m.) current-current correlator, Π_{em}. The latter can be written in terms of its longitudinal and transverse projections as

$$\Pi_{\mathrm{em}}(q_0,\boldsymbol{q}) = \frac{1}{3}\left[\Pi^L_{\mathrm{em}}(q_0,\boldsymbol{q}) + 2\Pi^T_{\mathrm{em}}(q_0,\boldsymbol{q})\right]\ , \quad (2)$$

both depending separately on energy and three-momentum. Below momentum transfers of about 1 GeV, the hadronic part of the e.m. current can be accurately saturated by the light vector mesons within the well-established vector dominance model (VDM). The correlator is then expressed through the imaginary parts of the vector meson propagators (= spectral functions) as

$$\mathrm{Im}\Pi_{\mathrm{em}} = \sum_{V=\rho,\omega,\phi} \frac{(m_V^{(0)})^4}{g_V^2}\mathrm{Im}D_V\ . \quad (3)$$

In the following we will neglect the small contributions from the isoscalar part and concentrate on the ρ meson which plays by far the most dominant role for the time scales involved in heavy-ion reactions.

Along the lines of our earlier analyses [8] the ρ propagator in hot hadronic matter,

$$D_\rho^{L,T} = \frac{1}{M^2 - (m_\rho^{(0)})^2 - \Sigma^{L,T}_{\rho\pi\pi} - \Sigma^{L,T}_{\rho M} - \Sigma^{L,T}_{\rho B}}\ , \quad (4)$$

is evaluated in terms of various contributions entering its in-medium selfenergy Σ_ρ. The meson gas effects (encoded in $\Sigma_{\rho M}$) are accounted for following [16] through interactions with the most abundant thermal π, K and ρ mesons saturated with a rather complete set of s-channel resonances R up to 1.3 GeV. The interaction vertices have been constrained by both hadronic ($R \to P\rho$) *and* radiative ($R \to P\gamma$) decay branchings. Also, the Bose enhancement for the in-medium $\rho\pi\pi$ width has been included in $\Sigma_{\rho\pi\pi}$.

The ρ modifications in nuclear matter are based on the model constructed in [8,17,18], where direct $\rho N \to B$ interactions (B=N, Δ, $N(1520)$, $\Delta(1700)$, $N(1720)$, ..., encoded in $\Sigma_{\rho B}$) as well as pion cloud modifications through πNN^{-1} and $\pi\Delta N^{-1}$ excitations (entering $\Sigma_{\rho\pi\pi}$) were calculated. Again, the model parameters have been thoroughly constrained by analyzing photoabsorption spectra on nucleons and nuclei as well as $\pi N \to \rho N$ scattering data. The latter enforce a rather soft form factor on the πNN vertex. Also, since the VDM is less accurate in the baryonic sector, an improved VDM coupling [19] has been employed for the (transverse) $\gamma N \to B$ transition form factors so that

$$\mathrm{Im}\Pi_{\mathrm{em}} = \frac{1}{3g^2_{\rho\pi\pi}}\left[\mathcal{F}^L + 2\mathcal{F}^T\right] \quad (5)$$

with

$$\begin{aligned}
\mathcal{F}^L &= -(m_\rho^{(0)})^4\ \mathrm{Im}D_\rho^L \\
\mathcal{F}^T &= -\mathrm{Im}[\Sigma^T_{\rho\pi\pi} + \Sigma^T_{\rho M}]|d_\rho - 1|^2 - \mathrm{Im}\Sigma^T_{\rho B}|d_\rho - r_B|^2 \\
d_\rho &= \frac{M^2 - \Sigma^T_{\rho\pi\pi} - \Sigma^T_{\rho M} - r_B\Sigma^T_{\rho B}}{M^2 - (m_\rho^{(0)})^2 - \Sigma^T_{\rho\pi\pi} - \Sigma^T_{\rho M} - \Sigma^T_{\rho B}}\ ,
\end{aligned} \quad (6)$$

cf. [9,17] (here $r_B^2 = 0.7$, the ratio between the actual γNB coupling and its value in the simple VDM).

At finite temperatures two additional features appear in the baryonic sector. Firstly, the Fermi-Dirac distribution functions are replaced by thermal ones [20, 8] which, at the temperatures of interest here ($T \simeq$

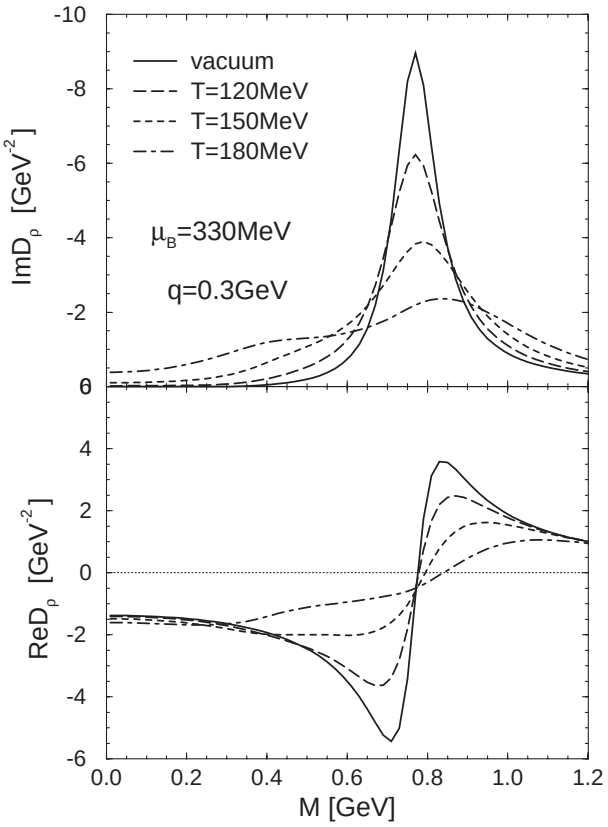

Fig. 1. Real (lower panel) and imaginary (upper panel) part of the ρ propagator in hot and dense hadronic matter at fixed baryon chemical potential $\mu_B = 330$ MeV and temperatures $T = 180$ MeV (corresponding to nucleon and total baryon densities of $\varrho_N = 0.67\varrho_0$ and $\varrho_B = 2.6\varrho_0$), $T = 150$ MeV ($\varrho_N = 0.25\varrho_0$, $\varrho_B = 0.72\varrho_0$) and $T = 120$ MeV ($\rho_N = 0.06\rho_0$, $\rho_B = 0.13\rho_0$)

150 MeV), are substantially smeared as compared to the zero-temperature Θ-functions. Secondly, a large fraction of the nucleons is excited into baryonic resonances which, in turn, are no longer active in nucleon-driven effects. However, as conjectured in [21], a baryonic resonance B_1 might still have excitations of type $\rho B_2 B_1^{-1}$ built on it. The particle data Table [22] indeed supports this hypothesis: e.g., the $\Sigma(1670)$ (which is a well-established four-star resonance with spin-isospin $IJ^P = 1\frac{3}{2}^-$), when interpreted as a $\rho\Sigma$ (or $\rho\Lambda$) 'resonance', very much resembles the quantum numbers and excitation energy ($\Delta E \simeq 500-700$ MeV) of the $\rho N \to N(1520)$ transition. In addition, the branching ratio of $\Sigma(1670)$ decays into 'simple' final states such as $N\bar{K}, \Sigma\pi$ or $\Lambda\pi$ is significantly less than 100%. Similar excitations on non-strange baryonic resonances are more difficult to identify as the latter themselves decay strongly via pion emission (i.e., the $B_2 \to B_1\rho$ decay is immediately followed by further $B_2 \to N\pi$ and $\rho \to \pi\pi$ decays). Nevertheless, from pure quantum numbers it is tempting to associate, e.g., $\Delta(1930)\Delta^{-1}$ or $N(2080)N(1440)^{-1}$ excitations with S-wave 'Rhosobar' states. We have conservatively estimated their coupling constants to give reasonable branching fractions into ρB_1 and γB_1 (the latter are typically in the range of 0.2–0.7 MeV). Due to the large total widths involved, their impact on the ρ propagator is weaker as compared to excitations on nucleons at equal densities; e.g., at T=150 MeV and $\mu_B = 436$ MeV, where, in chemical equilibrium, about 2/3 of the baryons are in excited states, the additional broadening from the calculated $B_2 B_1^{-1}$ excitations as compared to BN^{-1} ones amounts to about 40%. Concerning the pion cloud modifications, we do not explicitly compute the 'pisobars' on excited resonances but approximate their effect by using an effective nucleon density $\varrho_{eff} = \varrho_N + 0.5\varrho_{B^*}$.

The final result for the ρ spectral function in hot hadronic matter is displayed in Fig. 1 at fixed three-momentum and chemical potentials $\mu_\pi = 0$, $\mu_B = 330$ MeV for pions and baryons, respectively. One observes a strong broadening with increasing temperature and density. Comparing to the pure meson gas results of [16] (cf. Fig. 3 therein), it becomes clear that especially the low-mass enhancement around $M \simeq 0.4$ GeV is largely driven by baryons[1].

The pertinent three-momentum integrated dilepton production rates are shown in Fig. 2. At moderate temperature and density (upper panel), one still recognizes a remnant of the ρ peak, which, however, is entirely wiped out under conditions expected to be close to the phase boundary (lower panel). This provokes a comparison with quark-gluon based rate calculations, which, for simplicity, have been evaluated in terms of lowest order $O(\alpha\alpha_s^0)$ $q\bar{q}$ annihilation [23],

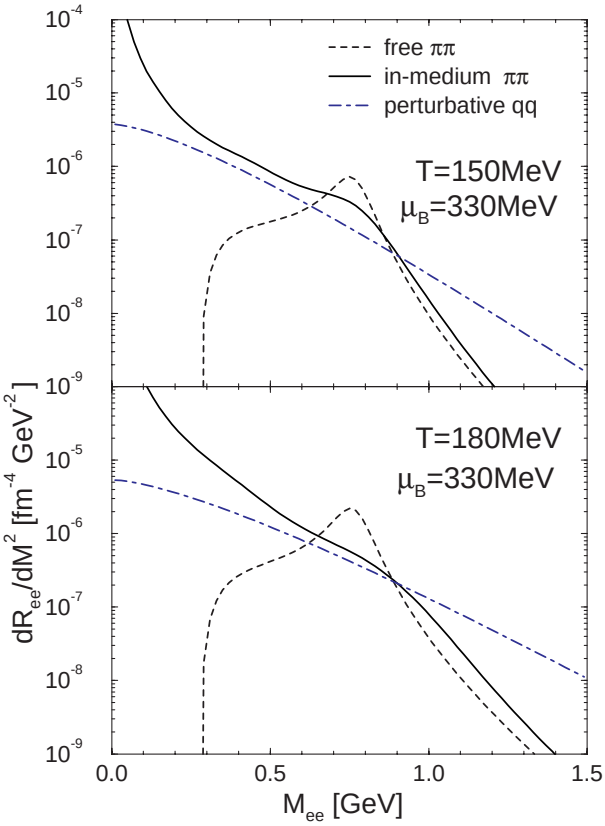

Fig. 2. Comparison of hadronic and partonic dilepton production rates (integrated over 3-momentum) in hot and dense matter at fixed baryon chemical potential (and equivalent quark chemical potential μ_q=$\mu_B/3$) for T=150 MeV (upper panel) and T=180 MeV (lower panel); dashed and full lines: $\pi\pi$ annihilation using the free and the in-medium ρ spectral function, respectively; dashed-dotted lines: lowest-order quark-antiquark annihilation

$$\frac{dR_{q\bar{q}\to ee}}{d^4q} = \frac{\alpha^2}{4\pi^4}\frac{T}{q} f^B(q_0;T) \sum_q e_q^2 \times \ln\frac{(x_- + y)\,(x_+ + \exp[-\mu_q/T])}{(x_+ + y)\,(x_- + \exp[-\mu_q/T])} \qquad (7)$$

with $x_\pm = \exp[-(q_0 \pm q)/2T]$, $y = \exp[-(q_0 + \mu_q)/T]$. In the vacuum the $q\bar{q}$ rates are known to coincide with the hadronic description for invariant masses $M \geq 1.5$ GeV as marked by the cross section ratio $\sigma(e^+e^- \to hadrons)/\sigma(e^+e^- \to \mu^+\mu^-)$ for the inverse process of e^+e^- annihilation (up to additional resonance structures in the vicinity of heavy-quark thresholds such as $c\bar{c}$). It seems that the in-medium hadronic rates indeed approach the partonic ones rather quickly leading to an approximate agreement at the highest temperatures/densities for masses of about 0.5–1 GeV (the deviation at masses $M > 1$ GeV is due to the incomplete description of the vector correlator in vacuum which does not include more than two-pion states; the discrepancy at low masses might be reduced once higher order α_S corrections are included, in particular soft Bremsstrahlung-type processes). A tempting interpretation of this behavior is a lowering

[1] With respect to the conditions realized in URHIC's at the full SpS energy (160-200 AGeV) this statement has to be taken with care as finite pion chemical potentials might arise towards freezeout which enhances the contributions from the meson gas.

of the 'quark-hadron duality threshold' in hot and dense hadronic matter. We will return to this issue in the discussion in Sect. 4.

3 Low-mass dilepton observables in Pb(158 AGeV)+Au

For a sensible application of the in-medium vector correlator to calculate dilepton production in URHIC's a realistic temperature and density profile is required. Microscopic transport or hydrodynamical simulations, e.g., have proven very successful in describing the final hadron observables. However, the associated dilepton yields, based on identical production rates, may differ appreciably [24], cf., e.g., [25] and [26]. As we will show below, a possible origin of this discrepancy might be related to the build-up of a finite chemical potential, which is usually not included in most hydrodynamical calculations to date (see, however, [27,28]).

Recent hadro-chemical analysis [13,14] of a large body of hadronic heavy-ion data has shown that the finally observed particle abundances at SpS energies are consistent with a common *chemical* freezeout at temperatures/baryon chemical potentials around $(T,\mu_B)_{ch} = (175,270)$ MeV. In the subsequent expansion and cooling the system is still strongly interacting with elastic collisions maintaining thermal equilibrium until the *thermal* freezeout. The absence of pion-number changing (inelastic) reactions (which is well supported phenomenologially from the inelasticities in $\pi\pi$ scattering) then induces a finite pion chemical potential [15]. To incorporate these features, we here take recourse to a simple expanding thermal fireball model. We start by generating a (non-interacting) resonance gas equation of state of hot hadronic matter including the lowest 32 (16) mesonic (baryonic) states. Imposing entropy and baryon number conservation determines the temperature dependence of the baryon chemical potential, $\mu_B(T)$. The additional requirement of pion- [kaon-] number conservation generates a finite $\mu_\pi(T)$ [$\mu_K(T) \simeq \mu_{\bar K}(T)$], with the various baryon chemical potentials kept in relative equilibrium (with respect to strong interactions), e.g., $\mu_\Delta(T) = \mu_N(T) + \mu_\pi(T)$, etc.. With an entropy per baryon of $s/\varrho_B = 26$, our trajectory is found to pass through $(T,\mu_N) = (175,250)$ MeV, compatible with the experimentally deduced point [13] (here, a small $\mu_\pi \simeq 20$ MeV is needed to be consistent with the final pion-to-baryon ratio of about 5:1 at SpS energies). Towards thermal freezeout at $(T,\mu_N)_{fo} \simeq (110-120, 415-450)$ MeV, $\mu_\pi(T)$ and $\mu_K(T)$ increase approximately linearly to around 80 and 110 MeV, respectively. Finally we need to introduce a time scale to obtain the volume expansion. We approximate the latter by a cylindrical geometry as

$$V_{FC}^{(2)}(t) = 2\ (z_0 + v_z t + \frac{1}{2}a_z t^2)\ \pi\ (r_0 + \frac{1}{2}a_\perp t^2)^2 \qquad (8)$$

employing two firecylinders expanding in the $\pm z$ direction. Guided by hydrodynamical simulations [28] the primordial longitudinal motion for Pb(158 AGeV)+Au reactions is taken to be $v_z = 0.5c$, and the longitudinal and transverse acceleration are fixed to give final velocities $v_z(t_{fo}) \simeq 0.75c$, $v_\perp(t_{fo}) \simeq 0.55c$ as borne out from experiment (this, in turn, requires fireball lifetimes of about $t_{fo} = 10-12$ fm/c and implies transverse expansion by 3-4 fm, consistent with HBT analyses [29]). The parameter r_0 denotes the initial nuclear overlap radius, e.g., $r_0 = 4.6$ fm for collisions with impact parameter $b = 5$ fm and $N_B \simeq 260$ participant baryons. The parameter z_0 is equivalent to a formation time and fixes the starting point of the trajectory in the (T,μ_N) plane.

With the such specified space-time evolution for ∼30% central Pb(158 AGeV)+Au collisions the dilepton yields from in-medium radiation are obtained as

$$\frac{d^2N_{ee}}{d\eta dM} = \frac{\alpha^2}{\pi^3 g_{\rho\pi\pi}^2 M}\int_0^{t_{fo}} dt\ V_{FC}^{(1)}(t)\int\frac{d^3q}{q_0} f^\rho(q_0;\mu_\varrho(t),T(t)) \times\mathcal{F}(M,q;\mu_B(t),\mu_\pi(t),T(t))\ Acc(M,\boldsymbol{q}) \qquad (9)$$

with $Acc(M,\boldsymbol{q})$ accounting for the experimental acceptance cuts (as well as an approximate mass resolution) in the '96 CERES data. The backward firecylinder is placed at a rapidity $y = 2.6$ to ensure the correct charged particle multiplicity as quoted by CERES. The electromagnetic 'transition form factor' $\mathcal{F}$ contains the in-medium ρ spectral function as described above, where the additional effects of the finite meson chemical potentials have been implemented in Boltzmann approximation. For initial conditions $(T,\varrho_B)_{ini}$=(190 MeV,2.55ϱ_0) and a freeze-out at $(T,\varrho_B)_{fo}$=(115 MeV,0.33ϱ_0) the fireball lifetime amounts to about t_{fo}=11 fm/c, see also above (reducing, e.g., $(T,\varrho_B)_{ini}$ to (180 MeV,1.92ρ_0) reduces the dilepton signal from the fireball by about 15%).

In addition to the in-medium radiation described by (9) the finally observed dilepton spectra contain a sizeable contribution from free hadron decays after freezeout, the so-called 'cocktail'. For this we employ the most recent evaluation of the CERES collaboration [31], which is generated from particle abundances based on the chemical freezeout of [13] being consistent with our (T,μ_B) trajectory. As in our previous works [8,32] the ρ-meson decays have been excluded from the cocktail as, owing to the short lifetime of the ρ, they are accounted for through the in-medium part, (9), in the vicinity of the (idealized) 'freezeout'.

The final results for the inclusive invariant mass spectra, shown in Fig. 3, demonstrate that the use of the in-medium spectral function leads to a reasonable agreement with the '96 CERES data, which cannot be described assuming vacuum ρ properties. This is in line with the conclusions of our earlier analysis [8], but we emphasize again that the results presented here are based on a much improved understanding of both the microscopic ρ spectral function (being constrained by a large body of independent data) as well as the space-time evolution dynamics (consistent with chemical freezeout analyses, without the use of an overall normalization factor, etc.). As compared to [8] the smaller μ_B in the early stages, the finite μ_π in

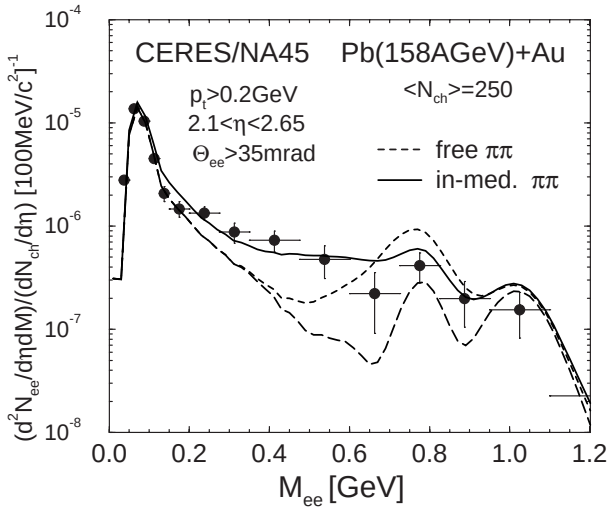

Fig. 3. 1996 CERES/NA45 inclusive dielectron invariant mass spectra from 30% central Pb(158 AGeV)+Au collisions [30] compared to the hadronic cocktail [31] (without ρ decays, dashed-dotted line) and to the cocktail plus $\pi\pi$ annihilation from the hadronic fireball using either the free (dashed line) or the in-medium (solid line) ρ spectral function from (4)

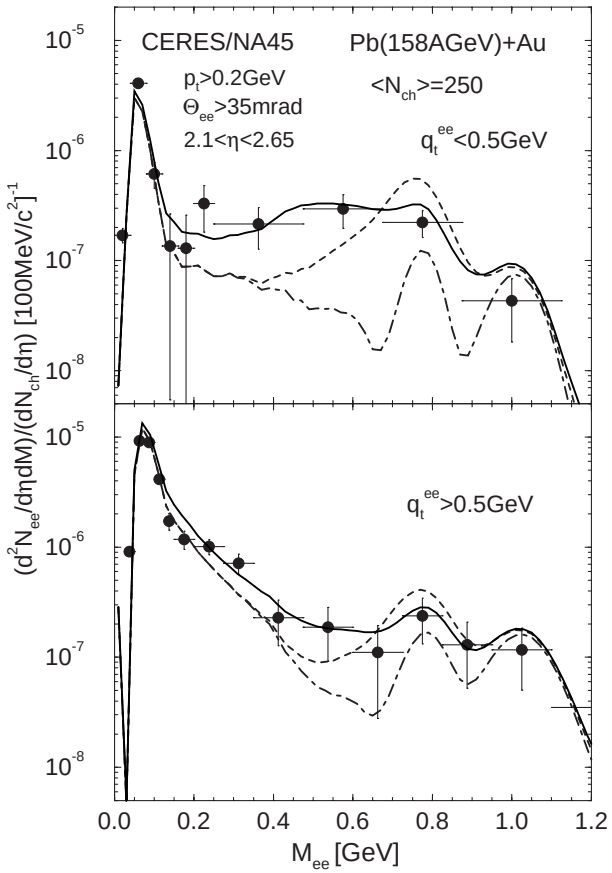

Fig. 4. Same as Fig. 3, but split into two transverse momentum bins below (upper panel) and above (lower panel) q_t=0.5 GeV

the later stages, and the more complete assessment of the meson gas effects [16] reduces the dominant role of the baryonic contributions to about equal importance as the mesonic ones. Another noteworthy point is that the overall dilepton yield exceeds what has been found in the hydrodynamical calculations of, e.g., [26] (where $\mu_\pi = 0$ has been used throughout) by about a factor of $\sim$2.5, thereby essentially resolving the above mentioned discrepancy to transport calculations [4,5].

A more detailed insight into the nature of the low-mass enhancement is revealed by inspecting its dependence on the transverse pair momentum q_t. Figure 4 shows the invariant mass spectrum seperated into two transverse momentum bins below and above $q_t = 0.5$ GeV. Clearly, the excess of the data over the free calculation is most pronounced in the small momentum bin which is properly reflected in our in-medium calculations. The same behavior is exhibited in another projection of the data in Fig. 5, where transverse momentum spectra in various invariant mass bins are displayed.

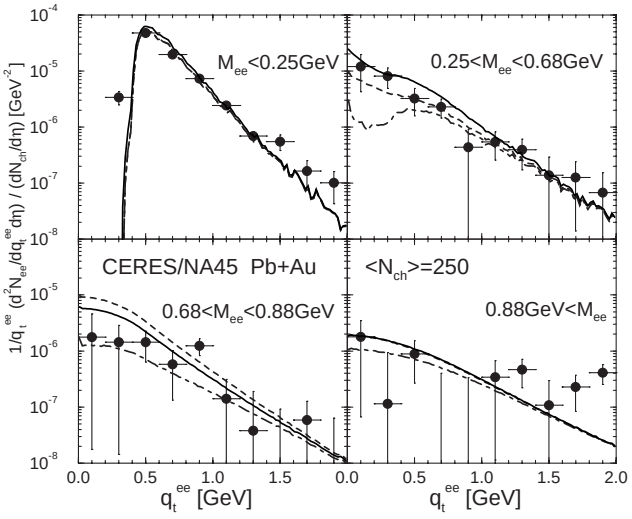

Fig. 5. 1996 CERES/NA45 transverse momentum spectra for e^+e^- pairs in 30% central Pb(158 AGeV)+Au collisions [30]. Line identification as in Fig. 3

4 Summary and discussion

Based on realistic hadronic interaction vertices we have shown that the in-medium ρ spectral function, evaluated within standard many-body techniques, undergoes a strong broadening in hot and dense matter. At comparable densities the baryonic effects prevail over mesonic ones due to the stronger nature of the meson-nucleon interactions. Corresponding thermal dilepton production rates exhibit a remarkable tendency to approach the lowest-order perturbative $q\bar{q}$ annihilation with increasing temperature and density. This might indicate the emergence of 'quark-hadron duality' towards the phase boundary down to rather low mass scales of 0.5 GeV, made possible through large imaginary parts resummed in the Dyson

equation of ρ propagator. The medium effects might thus be interpreted as a lowering of the 'duality threshold', which in free space is located around 1.5 GeV. An unambiguous identification of chiral restoration, however, requires the simultaneous treatment of the axial correlator (a_1 channel) which has to merge with the vector correlator which we have focused on here. Although the perturbative $q\bar{q}$ rate implies restored chiral symmetry, one has to keep in mind that (thermal) non-perturbative effects below 1 GeV are not yet well under control. The argument can be made more rigorous in the 1–1.5 GeV region, where the lowest-order in temperature mixing between vector and axialvector correlators suffices to establish a full degeneracy between them as well as the perturbatively calculated partonic result.

We have furthermore demonstrated that our model for the in-medium ρ spectral function is in line with current low-mass dilepton measurements at the CERN-SpS. For that we have employed a simple fireball expansion model consistent with recent hadro-chemical analysis and imposing effective pion-number conservation between chemical and thermal freezeout via finite pion chemical potentials (the latter seem to resolve a large part of the discrepancy in the total dilepton yield between transport and chemical equilibrium-based hydrodynamic simulations). The apparent depletion of the in-medium dilepton yield in the ρ/ω region, as well as the enhancement below can be accounted for. This also holds for the low-q_t nature of the excess. Upcoming high resolution measurements as well as the more baryon-dominated 40 GeV run will put the model predictions under further scrutiny and can be expected to advance our understanding of chiral symmetry restoration in hot and dense hadronic matter.

We are grateful for productive conversations with P. Braun-Munzinger, G.E. Brown, C. Gale, A. Drees, V. Koch, E.V. Shuryak, H. Sorge, H.-J. Specht and J. Stachel. We are especially indebted to A. Drees for providing us with the CERES cocktail. One of us (RR) acknowledges support from the Alexander-von-Humboldt foundation as a Feodor-Lynen fellow. This work is supported in part by the U.S. Department of Energy under Grant No. DE-FG02-88ER40388 and the National Science Foundation under Grant No. NSF-PHY-98-00978.

References

1. G. Agakichiev *et al.*, CERES collaboration, Phys. Rev. Lett. **75** (1995) 1272; P. Wurm for the CERES collaboration, Nucl. Phys. **A590** (1995) 103c
2. N. Masera for the HELIOS-3 collaboration, Nucl. Phys. **A590** (1995) 93c
3. G.E. Brown and M. Rho, Phys. Rev. Lett. **66** (1991) 2720
4. W. Cassing, W. Ehehalt and C.M. Ko, Phys. Lett. **B363** (1995) 35
5. G.Q. Li, C.M. Ko and G.E. Brown, Phys. Rev. Lett. **75** (1995) 4007; G.Q. Li, C.M. Ko, H. Sorge and G.E. Brown, Nucl. Phys. **A611** (1996) 539
6. J.V. Steele, H. Yamagishi and I. Zahed, Phys. Lett. **B384** (1996) 255; Phys. Rev. **D56** (1997) 5605
7. C. Song and V. Koch, Phys. Rev. **C54** (1996) 3218
8. R. Rapp, G. Chanfray and J. Wambach, Nucl. Phys. **A617** (1997) 472; G. Chanfray, R. Rapp and J. Wambach, Phys. Rev. Lett. **76** (1996) 368
9. B. Friman and H.J. Pirner, Nucl. Phys. **A617** (1997) 496
10. F. Klingl, N. Kaiser and W. Weise, Nucl. Phys. **A624** (1997) 527
11. W. Peters, M. Post, H. Lenske, S. Leupold and U. Mosel, Nucl. Phys. **A632** (1998) 109
12. R. Rapp and J. Wambach, "Chiral Symmetry Restoration and Dileptons in Relativistic Heavy-Ion Collisions", Adv. Nucl. Phys. in press, and hep-ph/9909**229**
13. P. Braun-Munzinger and J. Stachel, Nucl. Phys. **A638** (1998) 3c
14. J. Cleymans and K. Redlich, nucl-th/9903063
15. H. Bebie, P. Gerber, J.L. Goity and H. Leutwyler, Nucl. Phys. **B378** (1992) 95
16. R. Rapp and C. Gale, Phys. Rev. **C 60** (1999) 024903
17. R. Rapp, M. Urban, M. Buballa and J. Wambach, Phys. Lett. **B417** (1998) 1
18. M. Urban, M. Buballa, R. Rapp and J. Wambach, Nucl. Phys. **A641** (1998) 433
19. N.M. Kroll, T.D. Lee and B. Zumino, Phys. Rev. **157** (1967) 1376
20. R. Rapp and J. Wambach, Nucl. Phys. **A573** (1994) 626
21. G.E. Brown, G.Q. Li, R. Rapp, M. Rho and J. Wambach, Acta Phys. Polon. **B29** (1998) 2309
22. Particle Data Group, R.M. Barnett *et al.*, Phys. Rev. **D54** (1996) 1
23. J. Cleymans, J. Fingberg and K. Redlich, Phys. Rev. **D35** (1987) 2153
24. R. Rapp, Proc. of Quark Matter '99, Torino (Italy), May 10-15, 1999, and hep-ph/9907342
25. W. Cassing, E.L. Bratkovskaya, R. Rapp and J. Wambach, Phys. Rev. **C57** (1998) 916
26. P. Huovinen and M. Prakash, Phys. Lett. **B450** (1999) 15
27. B. Kämpfer, P. Koch and O.P. Paulenko, Phys. Rev. **C 49** (1994) 1132
28. C.M. Hung and E. Shuryak, Phys. Rev. **C57** (1998) 1891
29. U.A. Wiedemann, Proc. of Quark Matter '99, Torino (Italy), May 10-15, 1999, and nucl-th/9907048
30. G. Agakichiev *et al.*, CERES collaboration, Phys. Lett. **B422** (1998) 405; B. Lenkeit, Doctoral Thesis, University of Heidelberg, 1998
31. D. Irmscher, Doctoral Dissertation, Univ. Heidelberg 1993; T. Ullrich, Doctoral Dissertation, Univ. Heidelberg 1994; G. Agakichiev et al., CERES collaboration, Eur. Phys. J. **C4** (1998) 231; and A. Drees, private communication
32. R. Rapp, Proceedings of the 33rd Recontres de Moriond on "QCD and High Energy Hadronic Interactions", Les Arcs (France), March 21-28, 1998, published in Edition Frontiers, ed. J. Tran Thanh Van, and nucl-th/9804065